Using hyperspectral reflectance to detect different soil erosion status in the Subtropical Hilly Region of Southern China: a case study of Changting, Fujian Province

Chen Lin, Sheng-Lu Zhou & Shao-Hua Wu

Environmental Earth Sciences

ISSN 1866-6280
Volume 70
Number 4

Environ Earth Sci (2013) 70:1661-1670
DOI 10.1007/s12665-013-2253-y

Springer

Environ Earth Sci (2013) 70:1661–1670
DOI 10.1007/s12665-013-2253-y

ORIGINAL ARTICLE

Using hyperspectral reflectance to detect different soil erosion status in the Subtropical Hilly Region of Southern China: a case study of Changting, Fujian Province

Chen Lin · Sheng-Lu Zhou · Shao-Hua Wu

Received: 24 August 2011 / Accepted: 15 January 2013 / Published online: 3 February 2013

Abstract Hyperspectral reflectance is widely used for determining important properties of soil erosion. However, there have been few studies which focus on the influence of soil erosion intensity on the characteristics of hyperspectral reflectance, and such information would provide a new tool to improve quantitative understanding of soil erosion. In this study, 35 soil samples were collected from three regions with different erosion intensities in Changting County, a typical severely eroded county in the ferralic cambisol region of southern China, and classified into three groups according to different erosion controlling status. All the samples were scanned at wavelengths from 400 to 2,498 nm by an ASD Field Spec Portable Spectrometer, and the erosion intensity of each sample was calculated using the Revised Universal Soil Loss Equation. Multivariate stepwise linear regression was then employed to model the soil erosion intensity based on reflectance. The results suggested that the absorption peaks of each sample were in a similar wavelength range, while the absorption depth varied with different erosion status, and the reflectance of extremely eroded soil samples were the highest. During modelling of erosion intensity, the result was poor when all the samples were combined, but improved greatly at certain wavelength ranges when samples were classified into three groups based on different erosion controlling status. The extreme erosion group markedly outperformed the other two groups, in which the R^2 values between the actual and predicted erosion intensity were 0.67, 0.85 and 0.80 for each spectral type. The results indicated that hyperspectral reflectance is a promising method for accurately monitoring erosion intensity.

Keywords Hyperspectral · Soil erosion · Fe oxides · SOM · Erosion controlling status

C. Lin
State Key Laboratory of Lake Science and Environment, Nanjing Institute of Geography and Limnology, Chinese Academy of Sciences, 73 East Beijing Road, Nanjing 210008, People's Republic of China

S.-L. Zhou (✉) · S.-H. Wu
School of Geographic and Oceanographic Sciences, Nanjing University, Nanjing 210093, People's Republic of China
e-mail: zhousl@nju.edu.cn

Introduction

Soil erosion contributes about 85 % of total global land degradation. It not only breaks down land resources and gives rise to some significant environmental disasters, such as deposition, drought and flood, but also directly affects the sustainable development of regional ecological and social environments, exerting a dramatic influence on human habitat and economic development (Zhao and Shi 2007).

Since the 1960s, many studies have focused on soil erosion assessment by remote sensing; most of these extracted information from remote sensing images and modelled soil erosion intensity (Wischmeier and Smith 1965; Renard et al. 1997; Cox and Madramootoo 1998). These studies have provided useful results for soil erosion monitoring, but have always been limited by image resolution and subjective factors (Kouli and Soupios 2009). Increasing attention has therefore been paid to finding a better indicator of soil erosion to acquire accurate erosion information rapidly and effectively (Wells et al. 2007). Some studies demonstrate that topsoil spectra can meet this requirement because the spectral reflectance of eroded soil is significantly different from that of non-eroded soils

(Chappell et al. 2005; Bannari et al. 2006). Hyperspectral reflectance has been used widely to quantify soil properties in recent years, including important factors such as soil organic matter (SOM), heavy metals and chemical components (Montgomery 1976; Das 2007). Mathieu et al. (2007) found that the brightness and density of coarse fragments in soils could influence the spectral reflectance, and mapped soil erosion in a semi-arid Mediterranean environment (Coastal Cordillera of central Chile). Kooistra et al. (2001) used partial least squares (PLS) regression to establish the relationship between reflectance spectra in the visible–near-infrared region (VNIR) for spectrally active soil characteristics (SOM and clay contents) under laboratory conditions ($R^2 = 0.69$ and 0.92, respectively) for selected eroded soil in floodplains of the river Rhine in the Netherlands. Baumgardner et al. (1985) cited a study by Latz which showed that SOM and Fe_2O_3 were the most important factors for soil erosion. Normally, as erosion intensity increases, the Fe_2O_3 content increases and SOM decreases; such variations can be associated to changes in hyperspectral reflectance. The above reported results provide evidence that soil properties are closely related to soil erosion (Zhu and Lin 2011). However, there are some challenges remain. First, the quantitative relationship between the soil erosion modulus and reflectance spectra has rarely been studied. In most studies, soil erosion has always been characterised indirectly by some soil or environmental factors, while in fact the soil erosion modulus is widely recognised as the best indicator for directly reflecting erosion intensity. Price (1993) correlated the reflectance of the Landsat Thematic Mapper (TM) with the soil erosion modulus in Pinyon-juniper woodland in central Utah and found that the best correlation existed in Band 4 ($R = 0.88$); such a conclusion is very meaningful to further studies focusing on hyperspectral reflectance. Second, the study of sample classification is insufficient. In most studies, only calculation and validation samples were separated; however, it would be more useful to classify the samples according to erosion controlling status because the response of reflectance spectra varies with status (Kokaly et al. 2007). In this context, Lucas and Carter (2008) undertook a useful study to analyse the relationships between plant species richness and spectral indices derived from airborne hyperspectral image data. The correlation results showed that habitat types separated by five species were superior to the result for all habitat types combined.

The ferralic cambisol region in southeastern China is regarded as an important area for agricultural production. However, the irrational use of land has caused serious soil erosion and soil degradation, mainly made apparent in the loss of SOM and nutrients, acidification and enrichment of iron and aluminium oxide (Li 1989). In this study, hyperspectral properties were analysed in relation to the soil erosion controlling status in Changting County. The samples were collected from regions with different erosion intensities. The objectives of the study were to (1) determine the soil spectral characteristics under different erosion intensities, (2) establish the relationships between hyperspectral reflectance and soil erosion intensity, and (3) find a regression model to provide references for further studies.

Materials and methods

Study area

Changting County (25°18′40″N–26°02′05″N, 116°00′45″E–116°39′20″E) is located in western Fujian Province, China, covering an area of 320,000 hm^2. The research area represents a typical subtropical monsoon climate: it has characteristic wet (March–September) and dry (October–February) seasons. Severe weather is frequent. The average annual temperature is around 15–19 °C and the annual precipitation is 1,737 mm. There are many streams in the county, 17 of which are larger than 50 km^2. The majority of the land is woodland, with a small proportion of farmland. The dominant soil type of the county is ferralic cambisol, the main soil parent material is granite, and resistance to erosion is low.

Before the 1980s, some forest resources and native vegetation were cleared to favour agricultural production, which resulted in severe soil erosion in this area. According to available data, the total area of soil erosion in Changting was 97,469 hm^2 in 1983, which caused the county to be listed as an important pilot for erosion control in China. After a period of continuous effective control, the area of soil erosion decreased to 70,364 hm^2. However, due to imbalanced distribution of forest resources and conflicts between human activities and land protection, erosion is still a serious eco-environmental issue in the county. The areas suffering from soil erosion are widely found in granite hills and the centre of the county, which is intersected by many streams (Wang et al. 2005).

Soil sampling and classification

Top soils (0–10 cm) were sampled in April, 2010. The study area and sampling locations are shown in Fig. 1. According to field investigations, the soil type of all soil samples is hilly ferralic cambisols, the typical soil type in Southern China. A total of 35 soil samples were taken and classified into three groups based on their soil erosion controlling status: (1) extreme erosion ($n = 11$), characterised by the region having suffered a serious hill-collapse or erosion under pure masson pine trees, and with a soil

erosion modulus exceeding 10,000 mg ha^{-1} a^{-1}; (2) control in progress ($n = 12$), a region in which the technology and strategies applied were returning reclaimed land back into forests and grassland; and (3) control completed ($n = 12$), a region in which some orchards were planted and vegetation communities were restored, and thus currently soil erosion has been well controlled.

Methods

Quantitative assessment of soil erosion intensity

The soil erosion intensity transition in a spatial and temporal context was analysed using the Revised Universal Soil Loss Equation (RUSLE); the model as:

$$A = R \times LS \times K \times C \times P. \quad (1)$$

where A is the average soil loss due to water erosion (mg ha^{-1} a^{-1}), R is the rainfall and runoff erosive factor (MJ mm $ha^{-1}h^{-1}a^{-1}$), K is the soil erodibility factor (mg h MJ^{-1} mm^{-1}), L is the slope length (m), S is the slope steepness, C is the cover and management practice factor, and P is the support practice.

L, S, C and P were determined based on the remote sensing data and digital elevation model (DEM); L, S were calculated using the Spatial Analyst Tools in ArcGIS; C was taken to refer to vegetation coverage and was calculated using the Normalized Difference Vegetation Index (NDVI); P was determined according to Agriculture Handbook No. 703 of the United States Department of Agriculture (Renard et al. 1997), in which the land use types in the remote sensing images were firstly interpreted and then the P value distribution of various land use types was identified. R was calculated following an equation proposed by the Soil and Water Conservation Region Experimental Station of Fujian Province (Huang et al. 2004; Zeng and Pan 2007):

$$R = \sum_{i=1}^{12} (-1.5527 + 0.1792Pi) \quad (2)$$

where P_i is the monthly rainfall amount. The K value can generally be calculated by soil properties, using the Wischmeier's Erodibility Nomogram Equation (Wischmeier 1971). Ruan (1996) estimated the K values for different soil types using the above method, and these

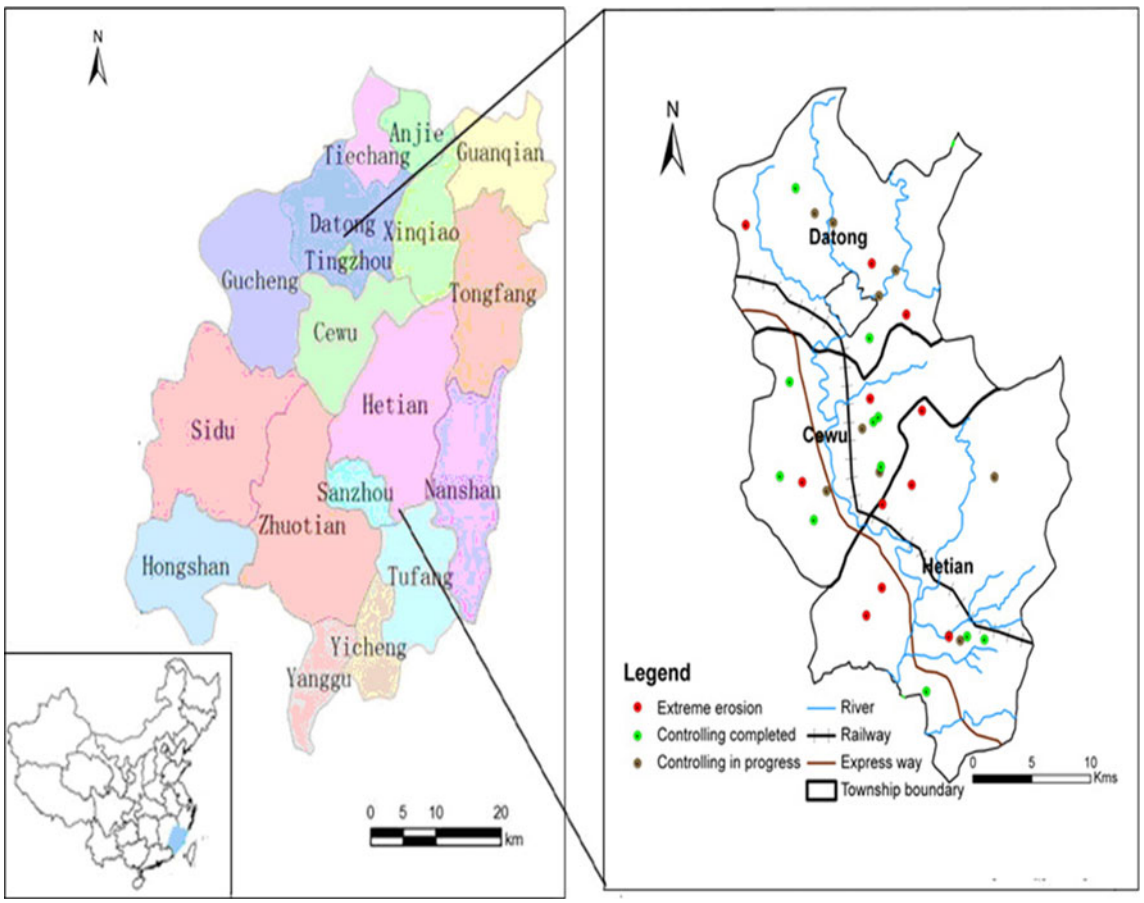

Fig. 1 Location of the study area, Changting County

figures were cited in this study. To facilitate the expression and calculation, the soil erosion modulus calculated by RUSLE was normalised so that the results ranged in [0, 1]; they were used to characterise soil erosion intensity of each pixel.

Reflectance measurements and hyperspectral analysis

Reflectance spectra were measured in a dark room, which allowed good control of irradiance conditions. Bidirectional spectral reflectance data over the 350- to 2,500-nm wavelengths were acquired using an ASD Field Spec Portable Spectrometer (Analytical Spectral Devices, Boulder, CO, USA) with a spectral resolution of 1.4 nm. The 8 °C field of view sensor was in the nadir position looking at the soil sample surface from a distance of 0.15 m, resulting in a field of view diameter of 2.1 cm, far less than the diameter of the tin (12 cm). To eliminate the influence of soil water content on the spectral curves, the samples were air dried before the hyperspectral measurements were taken. A 1,000-W halogen lamp situated at 0.70 m from the soil sample provided almost collimated rays over the sample area. The zenith angle of the lamp was set to 30 °C. This particular configuration was chosen to limit the influence of soil roughness by minimizing the fraction of shadow that could be observed. Reflectance was calibrated using a white spectrum on the panel. Each reflectance measurement produced a single spectrum. Four spectra were taken for each sample and the mean of the four spectra was taken as the actual reflectance of the sample (Liu et al. 2009).

To improve the validation of data, spectral data with a low signal-to-noise ratio of marginal bands at 350–390 nm and 2,451–2,500 nm were removed before the data were analysed, and the data smoothing was conducted using a Hamming window with a length of nine. Three spectral forms, including the original, first and second derivative spectra, were used for comparison (Xie et al. 2007). The estimated first derivative and second derivative spectra were used in Eqn. (3) and (4) as follows:

$$\rho'(\lambda_i) = [\rho(\lambda_{i+1}) - \rho(\lambda_{i-1})] / (\lambda_{i+1} - \lambda_{i-1}) \quad (3)$$

$$\rho''(\lambda_i) = [\rho'(\lambda_{i+1}) - \rho'(\lambda_{i-1})] / (\lambda_{i+1} - \lambda_{i-1}) \quad (4)$$

where λ_i is the wavelength, $\rho(\lambda_i)$ is the reflectance at λ_i, $\rho'(\lambda_i)$ and $\rho''(\lambda_i)$ are the first and second derivatives.

Model construction and validation

The correlations between reflectance of each spectral types and soil erosion intensity were initially analysed. As soil erosion intensity was dependent and each spectral method was independent, multivariate stepwise linear regression analysis was used to characterise soil erosion intensity with respect to the hyperspectral data. The F statistic was taken as the criterion of stepwise regression, in which F-enter and F-remove were set as 0.05 and 0.1, respectively (Chang and Laird 2002; Metternicht and Zinck 2010). The results were combined to compute the root-mean-square error (RMSE). The optimum number of terms was taken as the number resulting in the minimum RMSE.

Finally, to interpret the model results, the content of SOM in 35 samples was measured by wet digestion using an acidic solution of potassium dichromate with external heat and reflux condensers. The experimental results were further analysed to examine different hyperspectral responses of groups separated by different erosion intensities.

Results

Soil erosion intensity

To validate the soil erosion intensity calculated by RUSLE, the results were clustered by administrative districts. The correlation coefficient between erosion intensity of each rural and actual soil erosion modulus quoted from "Bureau of Planning of Soil and Water Conservation in Changting County (2007)" was analysed (Fig. 2). The result confirmed that RUSLE was a reliable and effective tool in soil erosion monitoring. The relationship between erosion intensity of 35 soil samples recorded in the field survey and the results calculated by RUSLE are shown in Table 1, with the erosion intensity for 32 samples within the calculated results. This confirmed the feasibility of sample classification based on erosion intensity.

The erosion intensity of three soil erosion groups was analysed by the statistical parameters of mean deviation,

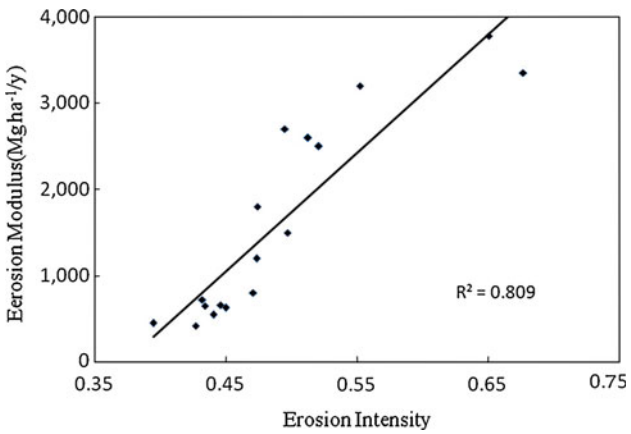

Fig. 2 Correlation between erosion intensity and erosion modulus of each village in Changting County

Table 1 Relationship between erosion intensity of recorded and calculated samples

Erosion intensity		*N*
Recorded	Calculated	
Extreme	Extreme	11
Control in progress	Control in progress	9
Control completed	Control completed	12
Control in progress	Extreme	2
Control in progress	Control completed	1

N The number of soil samples

Table 2 Descriptive statistical parameters of erosion intensity

Erosion status	*N*	Mean	SD	CV %
Extreme erosion	11	0.7916	0.1027	13
Control in progress	12	0.5784	0.2652	46
Control completed	12	0.2542	0.1372	53

N The number of soil samples

standard deviation (SD) and coefficient variation (CV) of erosion intensity (Table 2). As indicated by mean value, the value of the extreme erosion group was the highest, while there was little difference in values of the other two groups. The CV value for the "control completed" group and "control in progress" group was significantly higher than "extreme erosion" group, in relation to the variety of controlling measures present in this group.

Properties of reflectance spectral

The reflectance spectra of 35 samples after smoothing are shown in Fig. 3. The spectral continuum removed curves better illustrates the spectral absorption properties and are shown in Fig. 4.

The overall performance of the spectral curve showed low reflectance in the visible wavelengths, with increased reflectance towards the infrared. In near-infrared interval, reflectance was higher between 900 and 1,800 nm, but the overall spectral curve was steeper, and accompanied by expected variations. Meanwhile, spectra peaks of all the samples appeared to be fairly consistent; apart from the water absorption peaks generated by the –OH group vibration at 1,400 and 1,900 nm, the spectral curves still appear to have quite obvious absorption peaks at 500, 700, 950, 1,800, 2,200 and 2,300 nm with their corresponding ionic groups Fe^{2+}, Fe^{3+}, CO_3^{2-}, Al–OH and C–H, respectively (Ben-Dor 2002; Yan et al. 2003; Zhou et al. 2007). This indicates that iron oxides, organic matter and the aluminium complex have an important impact on soil spectra in the ferralic cambisol of southern China.

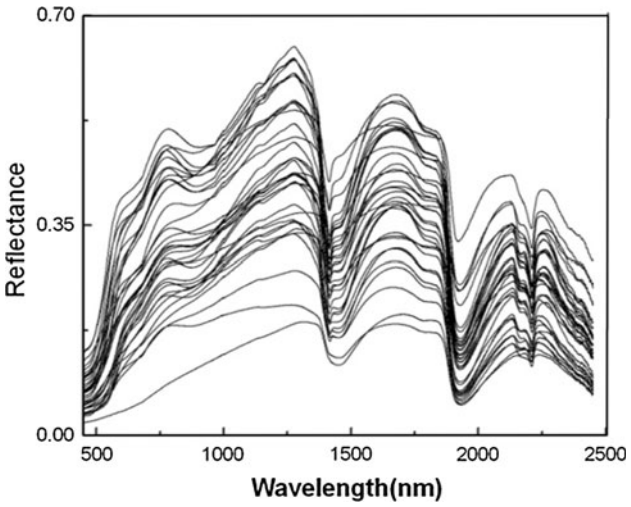

Fig. 3 Soil reflectance spectral curves

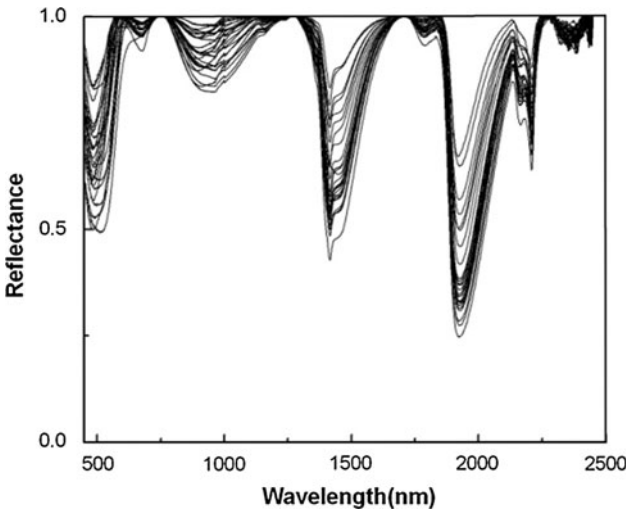

Fig. 4 Continuum-removed spectral curves

The differences of spectral curves in three groups (Fig. 5) indicate that the overall reflectance of the "extreme erosion" group was the highest, followed by "control in progress" and "control completed". To further distinguish the spectral curves, we compared the average reflectance of the three groups at 510, 780, 1,400, 1,875 (the most typical absorption wavelengths of Fe^{2+}, Fe^{3+}, –OH, H_2O), 1,700, and 2,300 nm (the typical absorption wavelength of C–H) (Fig. 6). A similar tendency was found that reflectance decreased when erosion control accelerated, especially in the wavelengths of 510 and 780 nm formed by the absorption of Fe^{2+} and Fe^{3+}, for which the reflectance of 510 nm in three erosion groups were 0.13, 0.09 and 0.06, respectively. For the other four wavelengths, the difference between the "extreme erosion" and "control in progress" groups was not significant as

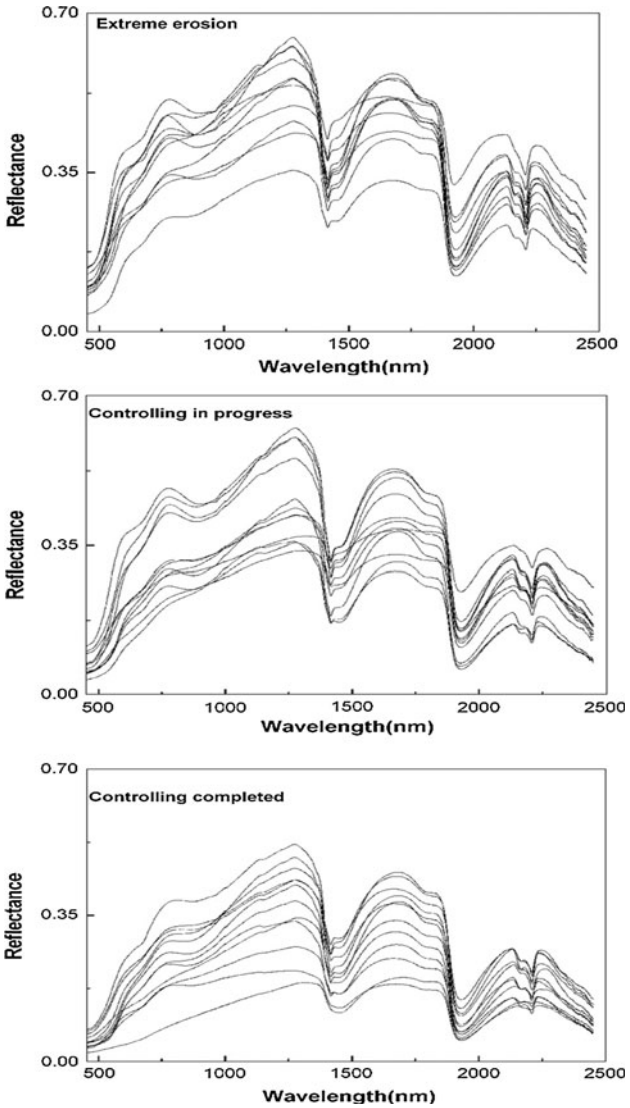

Fig. 5 Soil reflectance spectral curves classified by control situation

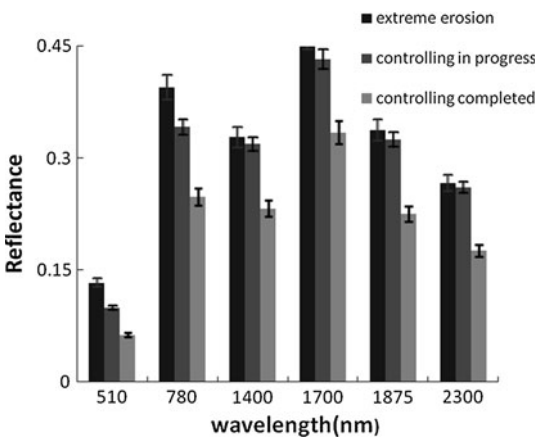

Fig. 6 The average reflectance of the three situations at characteristic wavelength

compared to that in 510 nm, while the "control completed" group was significantly lower than the former two.

These features show that, firstly, the average reflectance decreased as the governance progress accelerated, corresponding to the "control completed" group low value. Secondly, compared with C–H, H_2O and OH, Fe_xO_y seemed more sensitive to the differences among the three erosion intensities.

Correlation between spectral reflectance and erosion intensity

The correlation curves between spectral reflectance and erosion intensity are shown in Fig. 7. The correlation coefficient reached a high level at certain wavelengths in each erosion groups. In the "extreme erosion" group, the maximum value occurred at 1,130 mm (0.923), near to the absorption peak of Fe^{2+}. In the other two groups, the position of the maximum value was 1,957 mm (0.904), near to the absorption peak of Fe^{2+}, and 676 mm (0.891), near to the absorption peak of Fe^{3+}, respectively. This provided further evidence that iron oxides are sensitive to

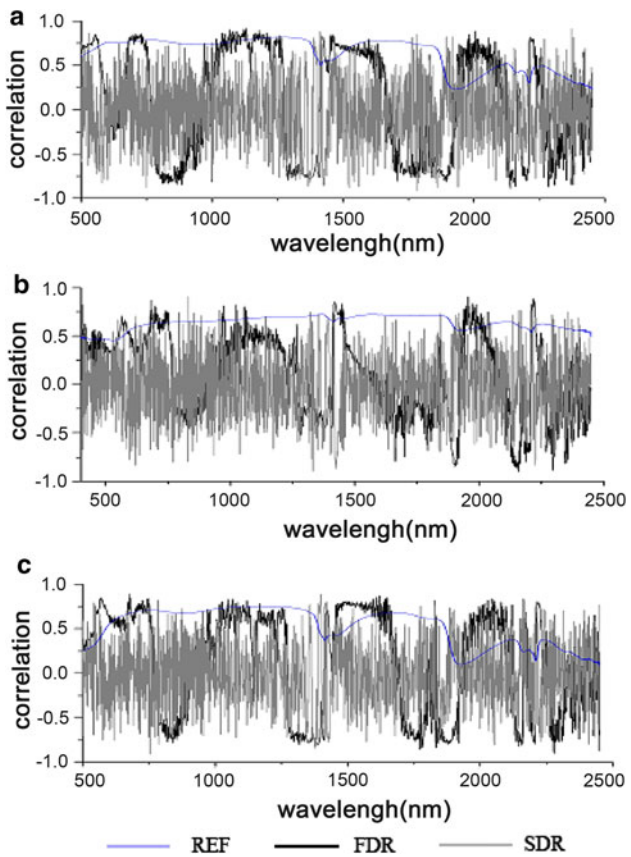

Fig. 7 Correlation coefficient between soil erosion intensity and the original, first and second derivative spectral reflectance. *REF* reflectance, *FDR* first derivatives reflectance, *SDR* second derivatives reflectance

Table 3 Descriptive statistics of correlation coefficients between hyperspectral reflectance and erosion intensity

Erosion situation	Max	Min	Mean	SD	CV, %
Extreme erosion	0.818	0.228	0.632	0.177	0.280
Control in progress	0.722	0.452	0.627	0.072	0.114
Control completed	0.747	0.089	0.507	0.214	0.421

the differences among three erosion intensity groups in the study area.

Comparing all the erosion intensity groups (Table 3) the maximal value of extreme erosion was 0.818, while the values in other two groups were lower than 0.75. The mean value of the first two subsets was higher than 0.62, with the value in the "extreme erosion" group being slightly higher, and that in the "control completed" group only 0.507. However, the values of SD and CV were different in the "control completed" group at 0.214 and 0.421, respectively, which was significantly higher than the other two groups. These results suggested that: erosion intensity of the "extreme erosion" group had the best correlation coefficient with hyperspectral reflectance; the curve of the correlation coefficient corresponding to "control completed" fluctuated dramatically and was mainly reflected in CV, SD and the range of values.

For each spectral type, the correlation coefficients corresponding to the original spectra in the visible spectral bands were slightly higher than those in the near infrared, which was attributed to the SOM and Fe oxides. This feature was more evident in "control completed" group and "extreme erosion" group (Fig. 7). In addition, the correlation coefficients corresponding to the spectra after deviation transformation were higher than coefficients corresponding to original spectra, in particular in the near-infrared bands (Fig. 7). The reason was that deviation spectra were able to highlight absorption characteristics that were hidden in the original spectra, the absorption of C–H (near to 2,300 nm) was a prominent example. The correlation coefficients of the first derivative spectra were higher than the second derivative spectra. For example, the maximal value for the "extreme erosion" group was 0.89 (676 nm), and the correlation coefficients for 44 wavebands were above 0.80 for all wavelengths. Regarding the other two spectral types, the number of indices exceed than 0.8 were 8 and 0, respectively. This feature was similar in "control in progress" and "control completed" groups.

Table 4 Descriptive statistics of modelling result (35 samples were combined)

Spectral method	Variables	R^2	RMSEP
REF	1	0.21	1.22
FDR	2	0.33	1.08
SDR	2	0.25	1.23

REF Original reflectance, *FDR* first derivative reflectance, *SDR* second derivative reflectance, *RMSEP* root-mean-square error of prediction

Modelling erosion intensity with spectral reflectance

When 35 samples were combined, the modelling result was poor (Table 4), which showed that the direct analysis of the relationship between soil erosion and spectral reflectance was unreliable, or even meaningless.

However, the results improved greatly when the samples were classified by each erosion control status (Table 5); it was noteworthy that the value of R^2 for "extreme erosion" was the highest, in which the values of the first and second derivative reached 0.8, even the lowest result for the original spectral was 0.67, while the other two groups were only 0.52 and 0.36, respectively. The R^2 of the "control completed" group was the lowest, in which the best value for the first derivative was only 0.63. For each spectral type, it was clear that the value for original spectra was lower than those for the other two spectra. Meanwhile, the difference between the first and second derivative was not significant and was uncertain; in "extreme erosion" and "control completed" groups, the value of R^2 with the first

Table 5 Simulation model of soil intensity in area of extreme erosion

Erosion status	Spectral method	Model	R^2	RMSE
Extreme erosion	REF	$I = 0.816 \times R\ (\lambda 1280) + 0.393$	0.67	0. 36
	FDR	$I = 651.86 \times R'\ (\lambda 1130) + 0.594$	0.85	0. 27
	SDR	$I = 338.52 \times R''\ (\lambda 2373) + 278.27 \times R''(\lambda 1412) + 0.653$	0.80	0. 13
Control in progress	REF	$I = 0.863 \times R\ (\lambda 1371) + 0.261$	0.52	0. 61
	FDR	$I = -228.34 \times R'\ (\lambda 682) + 210.26 \times R'\ (\lambda 1957) + 56.59 \times R'\ (\lambda 2216) + 0.415$	0.68	0. 42
	SDR	$I = 1937.48 \times R''\ (\lambda 831) + 0.261$	0.77	0.44
Control completed	REF	$I = 1.268 \times R\ (\lambda 1133) - 0.221$	0.36	0.31
	FDR	$I = 511.27 \times R'\ (\lambda 676) + 452.63 \times R'\ (\lambda 1621) - 0.203$	0.63	0.38
	SDR	$I = 1{,}573.33 \times R''\ (\lambda 1399) + 0.05$	0.56	0.36

Table 6 Descriptive statistical parameters of SOM

Erosion status	Samples (n)	Min (g kg^{-1})	Max (g kg^{-1})	Mean (g kg^{-1})	SD	Correl$^{\#}_{Re}$
Extreme erosion	11	1.69	14.42	6.49	4.31	-0.49
Control in progress	12	2.19	28.91	14.67	13.15	-0.56
Control completed	12	11.05	31.27	24.87	9.05	-0.76

$^{\#}$ Correlation coefficients between SOM and reflectance in visible spectral range (400–760 nm)

Table 7 Descriptive statistical parameters of vegetation coverage

Erosion status	Samples (n)	Min (%)	Max (%)	Mean (%)	SD
Extreme erosion	11	9.7	29.1	15.49	6.31
Control in progress	12	13.19	58.91	14.67	13.15
Control completed	12	48.05	79.05	63.44	9.05

derivative was better than that of the second derivative, in contrast to "control in progress" group.

To sum up, all the above results showed some features. First, the modelling result was best in the "extreme erosion" group, and worst in "control completed" group. Second, the modelling result of the original spectra was worse than the other two derivative spectral types. Thirdly, the RMSE of the models were very small, while not all of the R^2 results were satisfactory.

Discussion

Many soil properties, including SOM, H_2O, metal and clay have been modelled using hyperspectral reflectance in many previous studies (Ben-Dor and Banin 1995; Baumgardner et al. 1970), and gave good results (Ben-Dor et al. 1997; Goldshleger et al. 2001; Wu et al. 2005; Nduwamungu and Ziadi 2009). Therefore, as a comprehensive representation of such properties, erosion intensity was also demonstrated to form a relationship with hyperspectral reflectance. Interestingly, if all the samples were combined, the result was poor, while much better results were obtained when the samples were classified by erosion control status. As a result, it can be inferred that the lower interference resulting from different soil properties and high purity of soil samples were the key factors in establishing the optimal correlation between spectral reflectance and soil erosion intensity.

In the study area, SOM, H_2O, Fe and Al oxides can influence the spectrum to some extent (Croft et al. 2009). From the average reflectance in different wavelengths for each group (Fig. 6), it can be inferred that Fe oxides are the most direct and sensitive indicator for erosion intensity (510 and 780 mm). Therefore, to improve the correlation between the reflectance and erosion intensity, it was necessary to eliminate the interference of those factors on the spectrum. In this study, the samples were dried and ground before spectral measurements, and the influence of moisture, particle size and roughness could therefore be eliminated (Wu et al. 2007). In the context of SOM, when SOM content was higher than 2 %, organic matter could mask the influence of other factors on the spectral characteristics, especially in the visible light spectral range (Bowers and Hanks 1965). In contrast, a high content of Fe oxides can determine the soil spectral reflectance, which can mask organic matter influences on the spectral characteristics (Stoner and Baumgardner 1981). In the ferralic cambisols of southern China, the enrichment of Fe oxides can make this effect more notable (Huang and Liu 1989).

Based on the descriptive statistical parameters for SOM among 35 samples (Table 5), the "extreme erosion" group had the minimum SOM content, in which the maximum value was only 14.42 g kg^{-1}, and the correlation coefficients with reflectance in the visible range was only 0.49, which was also the lowest in the three groups. These results show that the influences of SOM on spectral reflectance were mostly eliminated, and Fe oxides can influence spectral reflectance directly. In the "control in progress" group, both the content and its correlation coefficients with reflectance in the visible range were significantly higher than the former, but lower than "control completed" group, while the SD was the highest (Table 6). Among the 12 samples in this group, five are close to mountains to facilitate forestation, and seven are exploring and reclaiming wasteland as orchards, with the undoubted result of improving soil erosion effectively; the situation was however different for SOM. In the early days of exploring and reclamation, decomposition of SOM was accelerated, and the quantity returned to the soil was therefore insufficient, so the SOM content varied greatly between samples in a given period (Li and Wang 1998). In addition, due to a long period of soil erosion, the surface soils in this group were almost completely stripped, the content of Fe and Al reached a high level because the deposition of metal is always beneath the topsoil. As a

result, the comparison between the content of Fe and SOM in soil samples was uncertain, and their relationships with spectral reflectance were also complicated, the correlation between spectral reflectance and soil erosion intensity was not at all optimal. In the "control completed" group, different control measures had different effects on soil properties. Of the 12 samples, five were controlled by vegetation recovery, which resulted in a litter of trees and fertilizer increasing the SOM content quickly; four were controlled by orchard construction, including complementary planting of Bahiagrass, Lespedeza and Partridge grass, which can greatly reduce the content of metal in soil and improve the SOM (Li 1999); three were controlled by compositing measures, which can improve the samples' ecological environment and accelerate the material circulation of SOM. Table 6 illustrates that the mean content of SOM can reach 20 g kg^{-1}. SOM's influence on spectral reflectance is much larger than in the other two groups, which led to the correlation result between spectral reflectance and soil erosion intensity being the worst of the three groups.

On the other hand, the surface soil with minimal vegetation coverage allowed hyperspectral curves of the bare soil to be obtained. The upward trend of vegetation coverage from "extreme erosion" to "control completed" is clearly shown in Table 7, which corroborates the conclusion that loss of sparse vegetation is the most intuitive embodiment of erosion soil (Shi et al. 2000).

Conclusion

This study divided the samples into three groups based on the different soil erosion control situations, and then analysed their reflectance spectra characteristics, finally establish the relationships between hyperspectral and soil erosion intensity.

The results showed that the absorption peaks appeared in similar wavelength ranges and varied with depth, that the "extreme erosion" group showed the highest reflectance of the three groups of different erosion controlling status, which certified that there is a relationship between hyperspectral reflectance and erosion intensity. The absorption peaks occurred near to 521, 951, 1,417, 1,937 and 2,208 nm, which suggested Fe^{2+}, Fe^{3+}, H_2O, Al–OH might have an influence on spectra, of which Fe oxides and SOM seemed to be the most sensitive factors to directly represent soil intensity in the study area.

When modelling erosion intensity, the result was poor when all the samples were combined. This improved when the samples were grouped into classes according to different erosion control status. The "extreme erosion" group markedly outperformed the other two groups, with the correlation (R^2) of the modelled results and erosion intensity for the three spectral types being 0.67, 0.85 and 0.80. This was due to the reduced influence of SOM and other soil properties on spectral reflectance. In conclusion, this study indicated that hyperspectral reflectance is a promising method for accurate monitoring of erosion intensity.

Acknowledgments Project was supported by key technologies for controlling remedy red soil degradation and developing high quality ecological agriculture (2009BADC6B).

References

Bannari A, Pacheco A, Staenz K, McNairn H, Omari K (2006) Estimating and mapping crop residues cover on agricultural lands using hyperspectral and IKONOS data. Remote Sens Environ 104:447–459

Baumgardner MF, Kristof S, Johannsen CJ (1970) Effects of organic matter on the multispectral properties of soils. Source Proc Indiana Acad Sci 79:413–422

Baumgardner MF, Latz K, Pazar SE, Van Scoyoc GE, Weissmiller RA (1985) Spectral characteristics in the monitoring of soil erosion. In: Soil Erosion and Conservation. Soil Conservation Society of America, Ankeny, pp 119–127

Ben-Dor E (2002) Quantitative remote sensing of soil properties. Adv Agron 75:173–243

Ben-Dor E, Banin A (1995) Near infrared analysis (NIRA) as a rapid method to simultaneously evaluate several soil properties. Soil Sci Soc Am J 59:364–372

Ben-Dor E, Inbar Y, Chen Y (1997) The reflectance spectra of organic matter in the visible near-infrared and short wave infrared region (400–2500 nm) during a controlled decomposition process. Remote Sens Environ 61(1):1–15

Bowers SA, Hanks RJ (1965) Reflection of radiant energy from soils. Soil Sci 100(2):130–138

Chang CW, Laird DA (2002) Near-infrared reflectance spectroscopic analysis of soil C and N. Soil Sci 167:110–116

Chappell A, Zobeck M, Brunner G (2005) Using on-nadir spectral reflectance to detect soil surface changes induced by simulated rainfall and wind tunnel abrasion. Earth Surf Proc Land 30:489–511

Cox C, Madramootoo C (1998) Application of geographic information systems in watershed management planning in St. Lucia. Comput Electron Agric 20:229–250

Croft H, Anderson K, Kuhn NJ (2009) Characterizing soil surface roughness using a combined structural and spectral approach. Eur J Soil Sci 60:431–442

Das B (2007) Reconstruction of historical productivity using visible–near infrared (VNIR) reflectance properties from boreal and saline lake sediments. Aquat Ecol 41:209–220

Goldshleger N, Ben-Dor E, Benyamini Y, Agassi M, Blumberg DG (2001) Characterization of soil's structural crust by spectral reflectance in the SWIR region (1.2 ± 2.5 μm). Terra Nova 13:12–17

Huang YF, Liu TH (1989) The relation between spectral reflectance characteristics and soil properties—a case of Southern China (in Chinese). Chin J Soil Sci 4(4):158–160

Huang JL, Hong HS, Zhang LP (2004) Study on predicting soil erosion in Jiulong River Watershed based on GIS and USLE (in Chinese). J Soil Water Conserv 18(5):75–79

Kokaly F, Rockwell BW, Haire SL, King TVV (2007) Characterization of post-fire surface cover, soils, and burn severity at the

Cerro Grande Fire, New Mexico, using hyperspectral and multispectral remote sensing. Remote Sens Environ 106:305–325

Kooistra L, Wehrens R, Leuven RSEW, Buydens LMC (2001) Possibilities of visible–near-infrared spectroscopy for the assessment of soil contamination in river floodplains. Anal Chim Acta 446:97–105

Kouli M, Soupios P (2009) Soil erosion prediction using the Revised Universal Soil Loss Equation (RUSLE) in a GIS framework, Chania, Northwestern Crete, Greece. Environ Geol 57:483–497

Li QK (1989) Development and prospect of soil science in China (in Chinese). Acta Pedol Sin 26(3):207–216

Li ZP (1999) The variation of soil organic matter content in red soil, cultivated land and the way to improve it (in Chinese). In: He YQ (ed) Red Soil Ecosystem Research, vol 5. China Agriculture Press, Beijing

Li ZP, Wang XJ (1998) Simulation of soil organic carbon dynamics after changing land use pattern in hilly red soil region (in Chinese). Chin J Appl Ecol 9(4):365–370

Liu HJ, Zhang YZ, Zhang B (2009) Novel hyperspectral reflectance models for estimating black-soil organic matter in Northeast China. Environ Monit Assess 154:147–154

Lucas KL, Carter GA (2008) The use of hyperspectral remote sensing to assess vascular plant species richness on Horn Island, Mississippi. Remote Sens Environ 112:3908–3915

Mathieu R, Cervelle B, Remy D, Pouget M (2007) Field-based and spectral indicators for soil erosion mapping in semi-arid Mediterranean environments (Coastal Cordillera of central Chile). Earth Surf Process Landf 32:13–31

Metternicht G, Zinck JA (2010) Remote sensing of land degradation: experiences from Latin America and the Caribbean. J Environ Qual 39:42–61

Montgomery OL (1976) An investigation of the relationship between spectral reflectance and the chemical, physical and genetic characteristics of soils. PhD dissertation, Purdue University, West Lafayette, Indiana

Nduwamungu C, Ziadi N (2009) Near-infrared reflectance spectroscopy prediction of soil properties: effects of sample cups and preparation. Soil Sci Soc Am J 73(6):1896–1903

Price KP (1993) Detection of soil-erosion within Pinyon-Juniper woodlands using thematic mapper (TM) data. Remote Sens Environ 45(3):233–248

Renard KG, Foster GR, Weesies GA, McCool DK, Yoder DC (1997) Predicting soil erosion by water: a guide to conservation planning with the Revised Universal Soil Loss Equation (RUSLE). Agriculture Handbook No. 703, USDA-ARS

Ruan FS (1996) Study on the classification of erosion intensity on granite slopes (in Chinese). J Fujian Normal Univ 12:81–90

Shi DM, Wei QP, Liang Y, Yang YS, Lv XX (2000) Study on degradation index system of eroded soils in Southern China (in Chinese). J Soil Water Conserv 14(3):1–9

Stoner ER, Baumgardner MF (1981) Characteristic variations in reflectance on surface soils. Soil Sci Soc Am J 45:1161–1165

Wang WM, Chen MH, Lin JL, Wu QQ, Bl Zhong, Yue H (2005) Monitoring soil and water loss dynamics and its management measures in Changting County (in Chinese). Bull Soil Water Conserv 25(4):73–77

Wells R, Prasad S, Römkens MJM (2007) Soil deformation and its spectral signature. Earth Surf Process Landf 32:786–793

Wischmeier WH (1971) A soil erodibility nomograph for farmland and construction sites. Soil Water Conserv 26:189–193

Wischmeier WH, Smith DD (1965) Predicting rainfall-erosion losses from cropland east of the Rocky Mountains. Guide for selection of practices for soil and water conservation. In: Agriculture Handbook, 282. US Government Print Office, Washington, DC

Wu YZ, Chen J, Ji JF, Tian QJ, Wu XM (2005) Feasibility of reflectance spectroscopy for the assessment of soil mercury contamination. Environ Sci Technol 39:873–878

Wu YZ, Chen J, Ji JF, Gong P, Liao QL, Tian QJ, Ma RH (2007) A mechanism study of reflectance spectroscopy for investigating heavy metals in soils. Soil Sci Soc Am J 71(3):918–926

Xie XL, Sun B, Hao HT (2007) Relationship between visible–near infrared reflectance spectroscopy and soil concentration of heavy metals (in Chinese). Acta Pedol Sin 44(6):982–993

Yan SX, Zhang B, Zhao YC, Zheng LF, Tong QX, Yang K (2003) Summarizing the VIS–NIR spectra of minerals and rocks (in Chinese). Remote Sens Technol Appl 18(4):191–201

Zeng HJ, Pan WB (2007) Soil erosion estimation by using RUSLE, Rs and GIS models in the Wubuxi Watershed, Fujian (in Chinese). J Saf Environ 7(5):88–92

Zhao QG, Shi XZ (2007) Overview of soil resources (in Chinese). Science Press, Beijing

Zhou W, Ji JF, Williams B, Chen J (2007) Determination of goethite and hematite in red clay by diffuse reflectance spectroscopy (in Chinese). Geol J China Univ 13(4):730–736

Zhu Q, Lin HS (2011) Influences of soil, terrain, and crop growth on soil moisture variation from transect to farm scales. Geoderma 163:45–54